IEEE Access
Multidisciplinary | Rapid Review | Open Access Journal

Date of publication xxxx 00, 0000, date of current version xxxx 00, 0000.

Digital Object Identifier 10.1109/ACCESS.2024.Doi Number

EMG-based Continuous Estimation of Index Finger Movements with Varying Interjoint Coordination Patterns by Modeling Musculoskeletal Dynamics

Trenton A. Gilstrap[1], Thanh Phan[1,2], Mada M. Alghamdi[1,2], and Sang Wook Lee[1,2,3,4], Member, IEEE

[1]Department of Biomedical Engineering, Catholic University of America, Washington, DC 20064 USA
[2]Center for Applied Biomechanics and Rehabilitation Research, MedStar National Rehabilitation Hospital, Washington, DC 20010 USA
[3]Rehabilitation Medicine Department, National Institute of Health, Bethesda, MD 20892 USA
[4]Department of Mechanical Engineering, Korea Advanced Institute of Science and Technology, Daejeon, Korea.

Corresponding author: Sang Wook Lee (e-mail: leesw@cua.edu).

This work was in part supported in part by the U.S. National Institute on Disability, Independent Living, and Rehabilitation Research under Grant 90REMM0001.

ABSTRACT Surface electromyography (EMG) is widely used for predicting kinematics of intended finger movements in applications including teleoperation. Generally, 'black-box' models with high complexity such as neural networks (NN) were used to improve prediction accuracy, which may not reproduce other important movement characteristics such as smoothness or kinematic similarity. The goal of this study is to develop a novel EMG-based approach that models impact of finger intersegmental dynamics to reproduce 'physiologic' characteristics of coordinated finger movements. Performance of the proposed dynamic model was compared with a polynomial model with the same level of complexity (no dynamics considered) and NN models, based on (A) simulation data from four musculoskeletal systems with varying parameters; and (B) experimental data from 10 subjects performing finger movements with four distinct coordination patterns. Performance of the proposed dynamic model in predicting simulated movements was significantly better than the polynomial model with the same level of complexity (18 parameters). In predicting experimental data, performance of the dynamic model was significantly better than that of the NN model of lower complexity (480 parameters), and similar to that of the NN model of higher complexity (2976 parameters). Furthermore, movement quality produced by the dynamic model, quantified by jerk (smoothness) and kinematic similarity, and its computational efficiency were significantly better than other models. The proposed technique, which captures the impact of musculoskeletal dynamics in a compact form, can accurately reproduce physiologic finger movements with a higher computational efficiency than existing models, thus could serve as a robust tool for teleoperation.

INDEX TERMS Surface electromyography, joint kinematics, finger, movement prediction, musculoskeletal modeling, biomechanics, teleoperation

I. INTRODUCTION

Surface electromyography (EMG) has been used in a wide range of applications of human-machine interface, including teleoperation [1-3], prosthesis control [4,5], and rehabilitation [6,7]. Pattern recognition techniques are commonly employed for the purpose of controlling powered orthoses or prostheses, which allow users to execute different tasks by classifying 'patterns' of the features extracted from multiple EMG channels [8,9]. Conversely, in the field of teleoperation, EMG signals were typically processed for continuous estimation of kinetic/kinematic information, such as joint angles or forces, which are then used for an 'online' control of robots to achieve a given task goal, such as the end-effector position control [10,11].

For decoding intended finger movements from the EMG signals, both approaches have different advantages and limitations. Pattern recognition or classification models

[8,9,12-19] can discern and predict user intents to perform different hand gestures or movements, allowing an intuitive prosthesis control of manipulative actions. However, since these models typically regard each movement/task as a single, fixed (isometric) 'class' to be recognized, little information regarding its kinematics during each task, such as spatiotemporal coordination of multiple joints, can be extracted or monitored. It is thus difficult to implement 'online' adjustment of device control during task performance. In contrast, models developed for continuous kinematic estimation [20-28] can compute finger joint angles from the EMG signals during movements, allowing more precise 'position' control of multi-joint robotic hands. However, most models were implemented to predict relatively simple movements, such as cyclic finger movements (i.e., concurrent extension/flexion of all joints [22,23]) or grasping movements of objects with different sizes/shapes [25-27]. It is thus unclear whether these models can predict more complex movement patterns of the fingers used in manipulative actions, which typically require different coordination patterns of distal (i.e., distal and proximal interphalangeal; DIP and PIP) and proximal (i.e., metacarpophalangeal; MCP) joints [29,30].

More importantly, as the current EMG-based models are mostly 'data-driven' in nature, which are built to minimize prediction errors in joint angles, it is unclear whether these models can also replicate/reproduce other physiologic characteristics of human movements. For instance, movements of the distal (DIP/PIP) and proximal (MCP) finger joints are constrained by biomechanical [31,32] or neural [29,33] couplings, which result in coordinated movements with specific angular velocity profiles [34]. Spatiotemporal characteristics of human movements are also regulated by smoothness constraints, typically achieved by minimizing the 3rd time-derivative of displacement ('jerk') [34], and providing smooth trajectories as target movements is important to achieve stable grasping and manipulation by robotic hands [35]. Additionally, kinematic characteristics such as velocity profiles are important to replicate in certain human-machine interaction applications such as teleoperation [36] or robotic surgery [37]. Such kinematic characteristics of the model-produced movements, however, have not been examined. While some models have considered muscle excitation-activation dynamics (e.g., Hill-type actuator) [38,39], they did not consider the dynamic impact of inertial and viscous/damping components as the joint angles were modeled as linear combinations of the computed muscle forces.

In addition, while "black-box" models such as artificial neural networks (typically used in kinematic prediction [20-28]) may accurately predict joint angles, the model structure is very complex, which makes it difficult to interpret the resulting models, or to discern importance of different 'predictors' (model inputs – in our case, EMG signals) and to explain how they are related to the outcome [38]. This limits the use of these models as a possible diagnostic tool, as the identified model parameters are difficult to interpret due to their complexity [40,41]. Few current models consider/incorporate finger musculoskeletal dynamics, which not only may help reproduce coordinated multijoint finger movements with a lower level of model complexity but also can capture or characterize different neuromechanical characteristics underlying variability in finger coordination patterns across subjects [42].

In this study, we developed a novel EMG-based approach to reproducing kinematics of various finger movements in order to address aforementioned limitations. As intended for teleoperation applications, we recorded and utilized both intrinsic and extrinsic hand muscle activation profiles. The proposed model computed the single- and double-time-integrals of the muscle activation profiles to account for dynamic impacts of passive impedance (stiffness/damping) and inertia on intersegmental dynamics, then incorporated them in movement prediction; we previously showed that passive impedance properties significantly affect multijoint finger movement patterns using *in vivo* electrical stimulation tests [43]. Performance of the newly-developed model was examined in predicting finger movements in manipulative actions, for which four elemental finger movements with distinct interjoint coordination patterns were performed by ten neurologically-intact subjects. Model performance (error) and kinematic characteristics of the model-prediction (smoothness and correlation with displacement and velocity profiles) were compared with those obtained by long short-term memory (LSTM) neural network models similar to the black-box models used in previous studies [25,26].

We hypothesized that the level of prediction accuracy achieved by the proposed model and the neural network (LSTM) models would be similar, despite the lower complexity of the proposed model. We also expected that more natural, physiologic movements will be achieved by the proposed model, which would be quantified by the correlation coefficients between the measured and model-predicted movements (similarity) and their maximum jerk values (i.e., smoothness).

II. METHODS

In this section, we first described the details of the structures of the proposed dynamic model (model 1) and other models (models 2 and 3A/3B), which were employed to provide a point of comparison (section II. A). We then provided details of the model validation processes, performed using the simulated (section II. B) and experimental (section II. C) data.

A. MODEL DEVELOPMENT

1) DYNAMIC MODEL (MODEL 1)

The proposed model was constructed from the dynamic equations governing segmental motions. Considering a segment controlled by *n* muscles, the equation is written as:

$$I\ddot{\theta} = -b\dot{\theta} - k\theta + r_1(\theta)f_1 + \cdots + r_n(\theta)f_n \quad (1)$$

where I is the mass moment of inertia, b the passive damping, k the passive stiffness, $f_1 \cdots f_n$ the muscle forces, and $r_1(\theta) \cdots r_n(\theta)$ their moment arms (n: number of muscles/EMG channels). This equation was used to model the impact of different segment parameters on the muscle force-movement relationship. First, to model a dominant impact of passive stiffness (such as in slow movements) on intersegmental dynamics, assuming that the moment arms do not change significantly along the movements, the equation (1) can be simplified to estimate joint angle $\hat{\theta}_1$:

$$k\hat{\theta}_1 \approx r_1 f_1(t) \cdots + r_n f_n(t)$$
$$\rightarrow \hat{\theta}_1 = \frac{1}{k}[r_1 f_1(t) \cdots + r_n f_n(t)] = \sum_{i=1}^{n} \frac{r_i}{k} f_i(t) \quad (2)$$

During fast movements, for smaller body segments such as fingers, the impact of passive damping b would be significantly larger compared to that of other terms (i.e., inertia or stiffness), resulting in $\hat{\theta}_2$:

$$b\dot{\hat{\theta}}_2 \approx r_1 f_1 \cdots + r_n f_n \rightarrow \hat{\theta}_2 = \sum_{i=1}^{n} \int_{t_0}^{t} \frac{r_i}{b} f_i(\tau) d\tau \quad (3)$$

In case that the inertial impact is dominant in generating dexterous finger movements that are relatively slow but require abrupt speed changes ($\hat{\theta}_3$):

$$I\ddot{\hat{\theta}}_3 \approx r_1 f_1 \cdots + r_n f_n \rightarrow \hat{\theta}_3 = \sum_{i=1}^{n} \iint_{t_0}^{t} \frac{r_i}{I} f_i(\tau) d\tau \quad (4)$$

Now, approximating joint movements as a weighted sum of stiffness, damping, and inertia terms:

$$\hat{\theta} \approx c_1\hat{\theta}_1 + c_2\hat{\theta}_2 + c_3\hat{\theta}_3$$
$$= \sum_{i=1}^{n} \frac{c_1 r_i}{k} f_i(t) + \sum_{i=1}^{n} \frac{c_2 r_i}{b} \int_{t_0}^{t} f_i(\tau) d\tau + \sum_{i=1}^{n} \frac{c_3 r_i}{I} \iint_{t_0}^{t} f_i(\tau) d\tau \quad (5)$$

Here, the weights (c_1, c_2, c_3) describes the relative contribution of the stiffness, damping, and inertia terms to the movement dynamics, which would differ across the movement types. Now converting the equation using muscle activation (obtained from the EMG channel i; $i = 1, ..., n$) $u_i(t)$:

$$\hat{\theta} = \sum_{i=1}^{n} \alpha_i u_i(t) + \sum_{i=1}^{n} \beta_i \int_{t_0}^{t} \omega(t-\tau) u_i(\tau) d\tau + \sum_{i=1}^{n} \gamma_i \iint_{t_0}^{t} \omega(t-\tau) u_i(\tau) d\tau \quad (6)$$

where $\omega(t-\tau) = e^{-c(t-\tau)}$ denotes an exponential window function describing temporal discount of muscle force [44]. Here c value was selected as 1. Using this model, the joint angle can be approximated by a linear combination of three basis functions: muscle activation profiles $u_i(t)$ and their weighted integral and double-integral terms ($\int_{t_0}^{t} \omega(t-\tau) u_i(\tau) d\tau$, $\iint_{t_0}^{t} \omega(t-\tau) u_i(\tau) d\tau$) (Fig. 1A).

In order to estimate the model parameter vector $\mathbf{p_k} = \{\alpha_1^k, \ldots, \alpha_n^k, \beta_1^k, \ldots, \beta_n^k, \gamma_1^k, \ldots, \gamma_n^k\}$ $(3n \times 1)$ for each of the three joint angles ($\boldsymbol{\theta_k}$; k = 1: DIP or distal interphalangeal joint, 2: PIP or proximal interphalangeal joint, 3: MCP or metacarpophalangeal joint), the EMG data are first processed to calculate the activation profile ($\boldsymbol{U}_{N_t \times n}$) and the weighted single- and double-integral profiles ($\boldsymbol{UI}_{N_t \times n}$, $\boldsymbol{UII}_{N_t \times n}$). Then the model parameter $\mathbf{p_k}$ for each joint angle $\boldsymbol{\theta_k}$ can be estimated by a least-square method:

$$\boldsymbol{\theta_k} = \mathbf{X} \cdot \mathbf{p_k} \rightarrow \mathbf{p_k} = (\mathbf{X}^{-1} \cdot \mathbf{X})^{-1} \cdot \mathbf{X}^{-1}\boldsymbol{\theta_k} \quad (7)$$

Here, $\mathbf{X} = [\boldsymbol{U}_{N_t \times n} \quad \boldsymbol{UI}_{N_t \times n} \quad \boldsymbol{UII}_{N_t \times n}]$ (N_t: number of time points; n: number of EMG channels)

- $\boldsymbol{U}_{N_t \times n} = [\boldsymbol{u}^1 \quad \ldots \quad \boldsymbol{u}^n]$, where $\boldsymbol{u}_i = [u_i(t_0) \quad \ldots \quad u_i(t_f)]^T$
- $\boldsymbol{UI}_{N_t \times n} = [\boldsymbol{ui}^1 \quad \ldots \quad \boldsymbol{ui}^n]$, where $\boldsymbol{ui}^i = \left[\int_0^{t_0} \omega(t-\tau)u_1(\tau)d\tau \ldots \int_0^{t_f} \omega(t-\tau)u_n(\tau)d\tau\right]^T$
- $\boldsymbol{UII}_{N_t \times n} = [\boldsymbol{uii}^1 \quad \ldots \quad \boldsymbol{uii}^n]$, where $\boldsymbol{uii}^i = \left[\iint_{t_0}^{t} \omega(t-\tau)u_1(\tau)d\tau \ldots \iint_{t_0}^{t} \omega(t-\tau)u_n(\tau)d\tau\right]^T$, and
- $\boldsymbol{\theta_k} = [\theta_k(t_0) \quad \ldots \quad \theta_k(t_f)]^T$

To provide a point of comparison, two types of different models (models 2 and 3) were also developed and tested, as described below. The second model (model 2) was an alternative mathematical model, which is not based on musculoskeletal dynamics but matches the complexity of the model 1 (i.e., number of model parameters: 18). The third type of models (model 3A and 3B) use long short-term memory (LSTM) neural networks that are commonly used in the EMG-based joint angle estimation [26,27,45,46].

2) POLYNOMIAL MODEL (MODEL 2)

The second model estimated joint angle as a weighted sum of muscle activation and their power terms (i.e., squared and square-root), which was designed to contain the same number of parameters (n=18) with the model 1. This was to ensure that the achieved accuracy by these models (1A/1B) was not simply due to their increased complexity (i.e., larger number of parameters) (Fig. 1B).

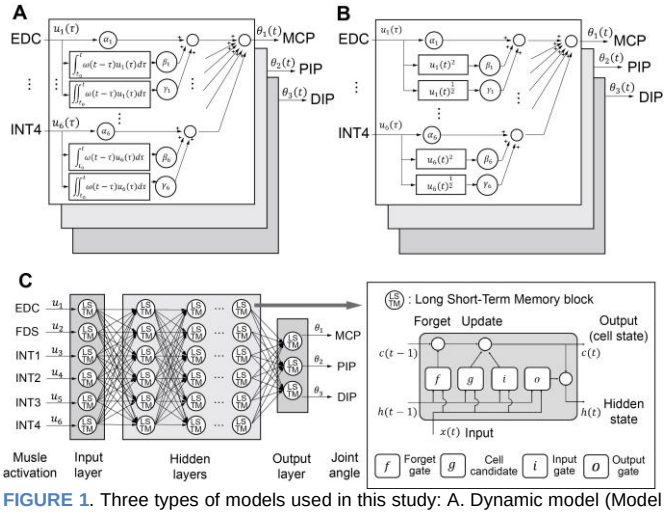

FIGURE 1. Three types of models used in this study: A. Dynamic model (Model 1); B. Polynomial model (Model 2); C. Long Short-Term Memory (LSTM) neural network model (Model 3A/3B).

$$\hat{\theta} = \sum_{i=1}^{n} \alpha_i u_i(t) + \sum_{i=1}^{n} \beta_i u_i(t)^2 + \sum_{i=1}^{n} \gamma_i u_i(t)^{\frac{1}{2}} \quad (8)$$

The basis functions used in this model (square and square-root) were determined by comparing accuracy of different polynomial basis functions, i.e., $u_i(t)^{1/2}$, $u_i(t)^2$, $u_i(t)^3$, $u_i(t)^4$, where we found that including higher-order terms (i.e., 3rd or higher) generally affect the accuracy negatively. The model parameters were then estimated by a

least-square method (similar to the dynamic model), as shown in the Eq. (7)

3) LSTM NEURAL NETWORK MODELS (MODEL 3A/3B)

The third type of models were developed using long short-term memory (LSTM) neural networks, commonly used in the EMG-based kinematic estimation models [26,27,42,43] (Fig. 1C). LSTM neural network models with two different levels of complexity were built to provide a point of comparison. The first model (model 3A) consists of two layers with eight hidden units (low-complexity), which include 480 parameters. The second model (model 3B) has 6 layers with 24 hidden units (high-complexity), resulting 2976 model parameters. For the network training, Adam optimization algorithm [47] was used, where the maximum number of epochs was set to 200 with the minimum batch size of 50. The initial learning rate was set to 0.01, and the dropout probability to 0.5.

B. MODEL VALIDATION: SIMULATION

First, performance of the dynamic model (model 1) and the polynomial model (model 2) was compared using a dataset generated by a simulation testbed (two-muscle system). The goal was to test efficacy of the model components proposed here (i.e., integral components of the model 1) in predicting dynamic relationships between the movement data and the EMG data recorded from the muscles. The simulated movement data contained sequential flexion and extension movements of a single joint, controlled by the agonist and antagonist muscles.

1) SIMULATION TESTBED: TWO-MUSCLE SYSTEM

A simulation model for a musculoskeletal system that consists of two muscles (agonist and antagonist) and a single joint was built in the MATLAB environment (MathWorks Inc., Natick, MA). This model produced movement data of sequential flexion and extension of the joint from a given anthropometric data (mass, joint impedance, etc.; see below) and muscle activation pattern. For the muscle activation, and corresponding EMG signals of the two muscles were also generated. The equation of motion of the segment controlled by two muscles is shown as below:

$$I\ddot{\theta} = -b\dot{\theta} - k\theta + r_1 f_1 + r_2 f_2 \qquad (9)$$

where θ is the joint angle, I the mass moment of inertia, b the passive damping, k the passive stiffness, f_1 and f_2 the agonist and antagonist muscle forces, respectively, and r_1 and r_2 the moment arms of the corresponding muscles. As described below ('Simulation' section), four sets of the anthropometric parameters were used to perform the simulation.

2) SIMULATION

Anthropometric parameters of the systems (mass moment of inertia, passive stiffness/damping) were selected to reflect typical finger segments [48,49], similar to those used in our previous study [43]. Four sets of different parameter values were used (Table 1) to simulate the movements of different musculoskeletal systems; system 1 adopted parameter values similar to those reported in the literature for the finger segments [43,48,49] while other systems (systems 2 – 4) represented systems with a 50% increase in joint damping (system 2), with a 50% decrease in joint stiffness (system 3), or with both changes (system 4).

TABLE I
ANTHROPOMETRIC DATA USED IN SIMULATION

System	I ($kg \cdot m/s^2$)	b ($N \cdot rad/s$)	k ($N \cdot rad$)	r_1 (m)	r_2 (m)
1	4×10^{-4}	8×10^{-3}	0.40	15×10^{-3}	12×10^{-3}
2		12×10^{-3}	0.40		
3		8×10^{-3}	0.27		
4		12×10^{-3}	0.27		

Sequential flexion and extension movements (duration = 4 seconds) were produced by activating the agonist muscle at t_{1i} = 1 (sec), then activating the antagonist muscle at t_{2i} = 3 (sec). The activation profile $u(t)$ for each muscle was simulated by a hyperbolic tangent function, using the rise time of approximately 0.5 (sec). A random noise was added to the signal, simulating the measurement noise, assuming a 10% signal-to-noise ratio.

Finally, the EMG data $e(t)$ for each muscle activation was simulated by taking the muscle force-to-EMG conversion dynamics [50-52], in which ζ value, the parameter that defines exponential curvature of the relationship between the EMG $e(t)$ and muscle force $u(t)$, was set to 0.01.

$$e_i(t) = 100\frac{e^{-\zeta u_i(t)} - 1}{e^{-100\zeta} - 1} \qquad (i = 1,2) \qquad (10)$$

3) DATA ANALYSIS

For each of the four systems with given anthropometric parameters (System 1 – System 4; Table 1), the system output (i.e., joint angular profile) was simulated from the EMG data computed from the given muscle activation pattern (Eq. 10). Then, the two models were used to reconstruct the joint angular profile from the muscle activation profiles. A root-mean-square error (RMSE) between the target and reconstructed movement profiles was computed as a measure of model accuracy, and a correlation coefficient (R-value) between the movement profiles as a measure of kinematic similarity [53].

C. MODEL VALIDATION: EXPERIMENT

Finally, performance of the developed models was evaluated against the experimental dataset obtained from healthy subjects who performed four types of finger movements.

1) SUBJECTS

Ten neurologically intact subjects (age: 31±5yrs) were recruited for the study. The experimental protocol was approved by the Institutional Review Boards at the Catholic University of America and the MedStar Health Research Institute, and informed consent was obtained from all subjects.

2) INSTRUMENTATION

To record muscle activity, six pairs of disposable, self-adhesive silver/silver chloride surface electrodes were used

to record electromyography (EMG) data from the extrinsic and intrinsic hand muscles (Fig. 2A/2B). Two pairs of electrodes were placed on forearm to record the extensor digitorum communis (EDC) and the flexor digitorum superficialis (FDS) activity, and four pairs of electrodes were placed on the dorsal and palmar aspect of the hand, which were intended to record activities of the intrinsic muscles that include the first dorsal interosseous (FDI), the second dorsal interosseous (SDI), the lumbrical (LUM), and the first palmar interosseous (FPI).

Once the electrodes were placed, the palm and the forearm were covered by self-adhesive wraps (Coban self-adhesive wrap, 3M company, MN, USA). Reflective markers to record finger movements were then placed on the dorsum of the hand, i.e., on fingertip, distal/proximal interphalangeal and metacarpophalangeal joints, and carpometacarpal joint of the index and middle fingers [54] (Fig. 2C). An 8-camera motion capture system (Optitrak Prime 13; NatrualPoint, Inc., OR, USA) was used to record marker movements at a sampling frequency of 100Hz.

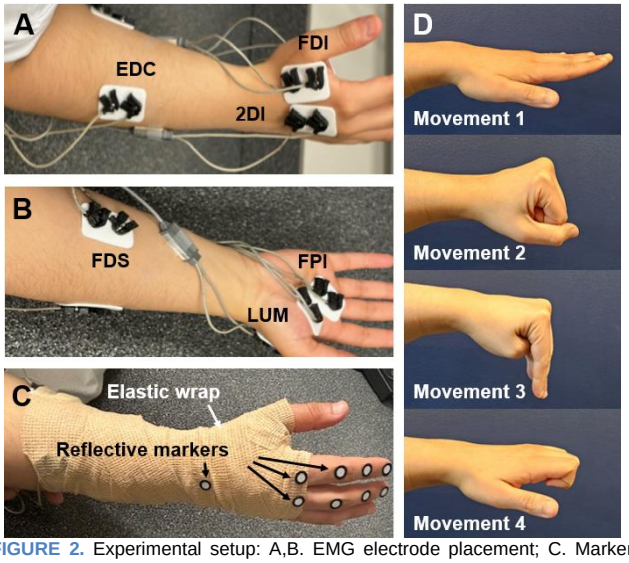

FIGURE 2. Experimental setup: A,B. EMG electrode placement; C. Marker placement; D. Target postures of the movements performed by subjects: extension (Movement 1) and flexion (Movement 2) of all joints, intrinsic plus (IP extension + MCP flexion; Movement 3), intrinsic minus (IP flexion + MCP extension; Movement 4). (IP: interphalangeal, MCP: metacarpophalangeal)

3) PROTOCOL

Once the electrodes and reflective markers were placed, subjects created maximum activations, for the normalization purpose, by performing the following movements: finger extension (EDC), finger flexion with the DIP joint extended (FDS), and index finger abduction (FDI).

Subjects performed four types of movements: Movement 1 - finger extension (IP and MCP extension); Movement 2 - finger flexion (IP and MCP flexion); Movement 3 - intrinsic plus (IP extension and MCP flexion); and Movement 4 - intrinsic minus (IP flexion and MCP extension) (Fig. 2D), which were performed at 2 different movement speeds (slow: 2-second duration, fast: 1-second duration). These four movements are elemental movements of the finger, which are employed in generating functional hand movements [55,56]. Intrinsic plus and minus movements are typically produced by activating exclusively the intrinsic muscles or the extrinsic flexor muscles, respectively [57].

Subjects rested their arm on a table, with their forearm in neutral position. A visual interface (LabView, National Instrument Corp., TX, USA) guided subjects to perform the target movement by providing information regarding timing of the movement. Five trials per each movement type and speed (total number of trials = 40) were recorded, and the order was randomized across subjects.

4) DATA ANALYSIS

Each of the three joint angles (DIP, PIP, and MCP) of the index finger was computed from the marker trajectories using a cosine law, then the initial angle was subtracted to obtain the change in joint angle measure. The EMG data was rectified, low-pass filtered (5Hz) to obtain the muscle activation profiles.

To evaluate performance of each model, the leave-one-out cross-validation method was used; given each trial (test dataset), the remaining four sets of the EMG and angle data (training dataset) were used to build the four models (Model 1, 2, 3A, and 3B), which were tested against the test dataset. Their performance was evaluated by a. Error; b. Similarity; c. Smoothness; d. Robustness; e. Computational cost.

a. Error: The prediction error was computed from the root-mean-squared error (RMSE) between the experimental data (joint angles) and their estimates from the EMG data by each model.
b. Similarity: The kinematic similarity between the experimental and model-produced movements was also computed. The coefficients of correlation (R) between the experimental and model-produced angular displacement and velocity profiles were estimated to quantify the similarity in the angular displacements and velocity kinematics.
c. Smoothness: The smoothness of the model-produced movements was evaluated by their maximum jerk values (i.e., 3rd time-derivative of the joint angles).
d. Model robustness: Between-trial variability in the model parameters was quantified by the Euclidean/Frobenius norm of the parameters across trials.
e. Computational cost: The computational time for each model computation was also recorded using the internal timer of MATLAB (tic/toc). A desktop computer with Intel® Core i7-1165G7 at 2.80GHz, with the internal memory (RAM) of 16GB was used for all simulation.

III. RESULTS

A. MODEL VALIDATION: SIMULATION

The model prediction results with the simulated flexion-extension movements indicated that the dynamic model (model 1), incorporating the single- and double-integral terms, reproduced more accurate prediction of the simulated angular profiles across all 4 systems (System 1 – 4) than the

polynomial model (model 2), as indicated by their RMSE values (Table II). The error magnitudes generally increased when the passive damping increased or when the passive stiffness decreased (Fig. 3). In particular, model 2 could not accurately predict the timing of the movement, as the timing of the predicted movement initiation generally precede that of the actual movement.

TABLE II
PREDICTION ERROR (RMSE) AND SIMILARITY IN ANGULAR DISPLACEMENT PROFILE (R-VALUE) FOR SIMULATION RESULTS

Measure	Model	System			
		1	2	3	4
RMSE (degrees)	1	0.25	0.20	0.36	0.56
	2	2.15	2.69	4.38	4.94
R-value	1	1.00	1.00	1.00	1.00
	2	0.98	0.98	0.97	0.96

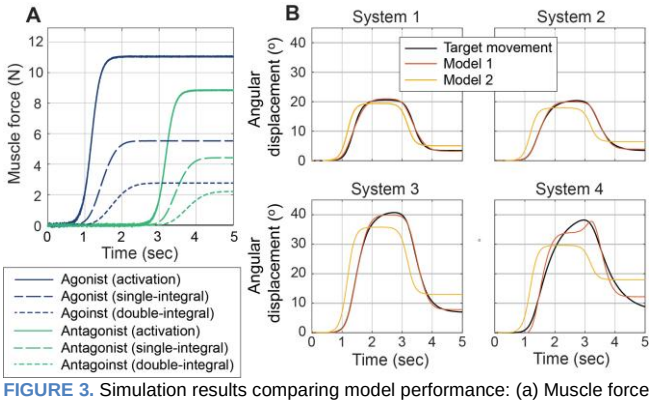

FIGURE 3. Simulation results comparing model performance: (a) Muscle force profiles used in simulation and their single- and double-integral profiles; (b1-b4) Simulated movements with four different sets of passive stiffness/damping values (System 1 – 4, as shown in Table I) and predicted movements by the two models (model 1 and 2) from the EMG profiles. The dynamic model (model 1) reproduced the movements more accurately across different parameter values, while accuracy of the polynomial model (model 2) degraded as the biomechanical properties of the model changed. Note that the simulated movements exhibited similar timing with the muscle activation integral profiles (A), especially when the magnitude of the passive damping is relatively greater than other parameters (i.e., System 4).

B. MODEL VALIDATION: EXPERIMENT

1) ACCURACY

Across all target movements, performance of the dynamic model (model 1) and the neural network model with high complexity (model 3B) was superior to the other models, as their prediction error values (RMSE) were significantly smaller than the other models (models 2 and 3A) for most of the movements (Fig. 4), which is also demonstrated in the representative case (Fig. 5).

2) PHYSIOLOGICAL MOVEMENT CHARACTERISTICS

Physiological characteristics of movements produced by model 1, evaluated by smoothness and kinematic similarity, were the closest to the experimental data when compared to all other models.

a. Maximum jerk (smoothness): The average maximum jerk values were the smallest for the dynamic model (model 1), while significantly larger jerk values were observed in the movements produced by the neural network models (model 3A/3B) (Fig. 6A). As shown in the representative case (Fig. 4), while models 1 and 2 produced relatively 'smooth' movements, the neural network models (model 3A/3B) often produced movements in which abrupt changes in the joint angle are observed. Such changes were typically amplified in time-derivatives (such as velocity, acceleration, and jerk) (see Fig. 5B), resulting in significantly larger average maximum jerk values (Fig. 6A).

b. Coefficient of correlation (kinematic similarity): The similarity of the predicted angular displacements to the actual movements, as quantified by the correlation coefficients (r-values), was the highest for the dynamic model (model 1) and the lowest for the polynomial model (model 2) (Fig. 6B). The between-model difference in the similarity was even greater for the angular velocity; the angular velocity profiles of the movements produced by model 1 showed the highest similarity to the measured velocity profiles compared to the other models (Fig. 6C), which can also be observed in the representative case shown (Fig. 5B). Note that the velocity profiles produced by all other models (models 2, 3A, and 3B) showed very weak correlation with the experimental data, as indicated by their small r-values (mean r-values < 0.2).

3) PARAMETER VARIABILITY

Variability in the model parameter values across trials was relatively low for the dynamic model (model 1: COV=0.8±0.5) and the polynomial model (model 2: COV=1.0±0.7), but the between-trial variability was significantly higher for the neural network models (models 3A: COV=1.4±0.2, model 3B: COV=1.4±0.1; all p-values < 0.001 when models 1 or 2 were compared to models 3A or 3B).

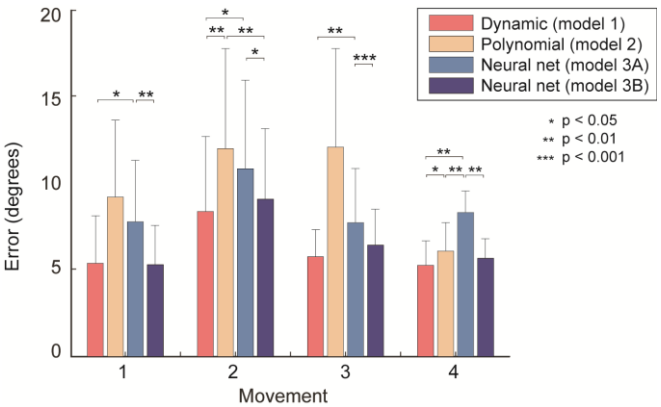

FIGURE 4. Prediction accuracy (error) of the four models during experimental validation. Overall, the dynamic model (model 1) and the high-complexity neural network model (model 3B) performed better than the other models.

4) COMPUTATIONAL COST

The computational cost was significantly greater for the neural network models, as their total computation time per trial (model 3A: 99.2±19.2seconds, model 3B: 120.5±7.1

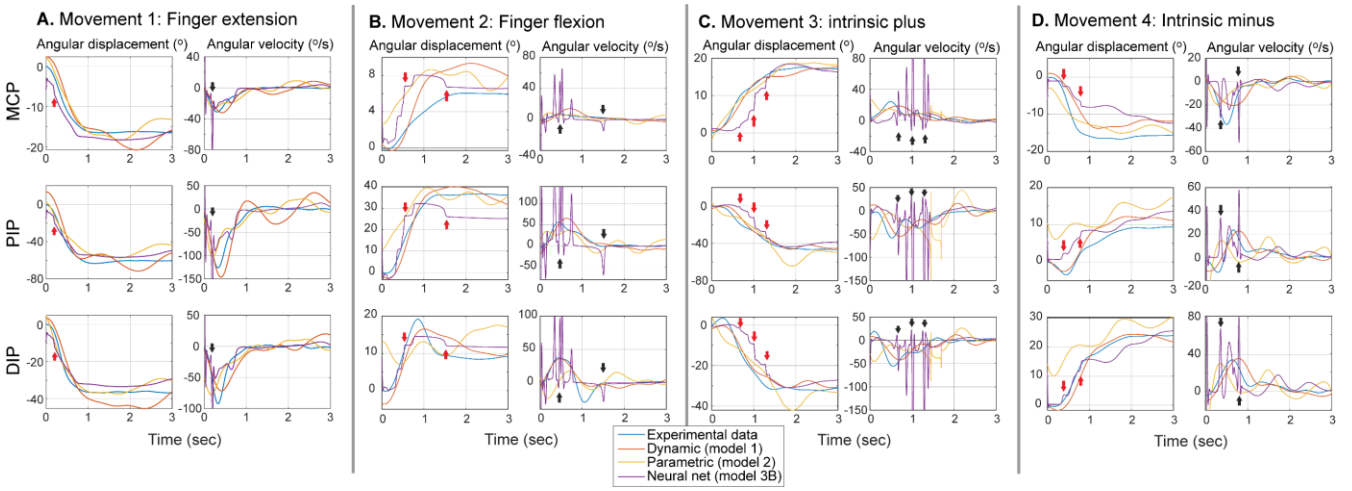

FIGURE 5. A representative case of model performance comparison (Subject 2) across four movement patterns (A-D). In general, the dynamic model (model 1; blue) and the neural net (NN) model with high complexity (model 3B; purple) predicted the angle profiles better than the parametric model (model 2; yellow). But the dynamic model (model 1) produced smoother and more physiologic movements than the NN model (model 3B); in particular, several cusps (sharp turns; red arrows) were observed in the movements produced by the NN model (model 3B), which resulted in even greater spikes in their derivatives (black arrows).

seconds) were considerably longer than those of the other two models (model 1: 0.7±0.1seconds, model 2: 0.7±0.1 seconds; all p-values < 0.001 when either models 1 or 2 were compared to models 3A or 3B).

IV. DISCUSSION

We demonstrate that the proposed dynamic model was capable of reproducing different functional hand movements from surface EMG data. In particular, this model was able to produce physiologic movements that exhibited high similarity to the angular displacement/velocity profiles of the measured (target) finger movements, with greater computational efficiency.

Our results emphasized the importance of using adequate basis functions for the EMG-based movement prediction; the proposed dynamic model (model 1) employed single- and double-integrals as basis functions, which can capture biomechanical impacts of the multisegmental dynamics (passive impedance). We observed that the single- and double-integrals of the muscle activation generally showed higher similarity to the measured finger movement profiles than the muscle activation profiles themselves. In particular, similar temporal characteristics were observed between the integral and the measured joint angles profiles (see Fig. 4), while the temporal profiles of the muscle activation generally do not match those of joint angle; note that the duration of the joint angle change (i.e., rise time) was often longer than that of muscle activation increase. Previous studies [43,54] demonstrated significant contribution of viscous torque (produced by passive damping) to finger movement production, which could explain the temporal delay between the muscle activation and the joint angle displacement. As the proposed dynamic model (model 1) utilized basis functions (i.e., activation integrals) that mimic dynamic behaviors of biomechanical components such as passive damping, it was able to achieve a comparable prediction accuracy with a significantly lower model complexity (i.e., fewer model parameters).

Furthermore, the proposed model has advantages over other models due to the 'physiologic' nature of its predicted movements, as quantified by the two kinematic parameters (i.e., smoothness and kinematic similarity) in this study. Note that previous EMG-based models developed for joint angle prediction [20-28,45,46] typically did not examine such movement qualities. In teleoperation, a reference movement trajectory should be 'smooth' to ensure proper manipulator control, such as maintaining stability in grasping/manipulation of the robotic hands [58]. Jerky finger movements could decrease grip stability, as seen in neurological disorders (e.g., Parkinson's disease; [59]). When these models are used for orthosis control (e.g., rehabilitation training), smooth and natural movements should also be used as a reference (target movement) to

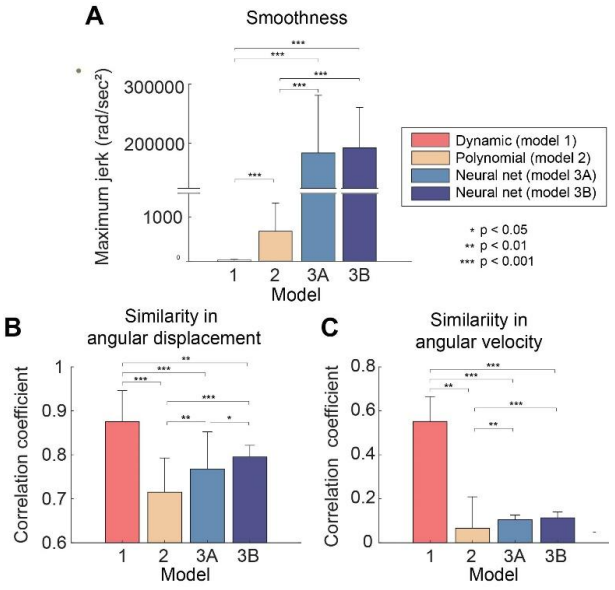

FIGURE 6. Movement characteristics of model-produced movements, averaged for all 4 movement types. A: Smoothness; B,C: Correlation between the experimental and predicted angular displacement (B) and velocity (C) profiles.

control hand orthosis as it would minimize the risks for injury during operation. The proposed dynamic model was also able to produce smooth movements with physiologic velocity profiles (i.e., highest similarity to the measured angular velocity profile), which is also important in hand-arm movement coordination [60,61]. Note that movement smoothness is also important in other possible human-robot interaction applications such as gesture recognition [62,63].

Finally, the proposed dynamic model also presents additional advantages over the other models due to its robustness and computational efficiency. The performance (i.e., RMSE) of the dynamic model were less sensitive to the trial chosen in the leave-one-out validation process, indicating it was less sensitive to the variabilities in the input data (i.e., less reliant on which trials are used for training). Also, the model may potentially serve as a diagnostic tool, as each model parameter defines the contribution of different biomechanical components (i.e., damping, stiffness, inertia) to finger movements. Finally, the proposed model presents unique advantage in the computational efficiency. The computational cost of the dynamic model (model 1) was almost negligible (computation time for each movement < 1 second) with a conventional desktop computer, compared to the computational time for the neural network models (models 3A and 3B) that was considerably higher (> 90 seconds).

Some limitations of the study are to be acknowledged. Activity of some deep hand muscles, such as the flexor digitorum profundus (FDP), were not measured by surface electrodes, which limit the amount of information required for movement prediction. However, previous study showed that the activities of two extrinsic flexor muscles (FDP and FDS) during functional task are highly correlated [64], thus some degree of information regarding FDP activities could have been deduced from the FDS activation pattern recorded in the study. The theoretical model used in our simulation (section III.A.) did not include complex nonlinear dynamics of other factors such as passive tendon stiffness or tendon force distribution within finger extensor mechanism [65] that affects finger movement production, which may explain the observed high similarity between movements (i.e., R-values ≈ 1). Our previous *in vivo* study [43], however, showed that theoretical models considering passive impedance, such as one described in (1), can reproduce multi-joint finger movements rather accurately, if produced at self-selected speed. Note that significant differences in performance between the models were captured by the absolute difference and/or error, i.e., RMSE measures, which showed that the proposed dynamic model can compute spatiotemporal patterns of multi-joint finger movements more accurately. We also recorded and used the intrinsic muscle activities, which are not available for amputees, making its applications limited to those involving non-amputees such as teleoperation. We also limited the scope of our model to the prediction of the index finger movements; prediction of multi-finger movements, however, can be performed in the future studies by adding more channels/electrodes recording other intrinsic muscles. However, recording of intrinsic muscle during orthosis control could be difficult (due to physical interference). Thus, pros and cons of using intrinsic hand muscles should be carefully considered.

V. CONCLUSION

In this study, we developed a novel dynamic model that can reproduce various functional hand movements from surface EMG data. The proposed model predicted finger movements with a level of accuracy comparable to that of complex neural network models. More importantly, the proposed model produced physiologic movements that exhibited high similarity to the angular displacement/velocity profiles of the measured finger movements, with greater computational efficiency. The proposed modeling approach thus provides a robust and computationally-efficient tool for human-machine interaction applications such as real-time prosthesis/orthosis control or teleoperation.

REFERENCES

[1] P. K. Artemiadis and K. J. Kyriakopoulos, "EMG-based teleoperation of a robot arm using low-dimensional representation," in *Proc. IEEE/RSJ Int. Conf. Intell. Robots Syst*., pp. 489-495. Oct. 29, 2007.

[2] P. K. Artemiadis and K. J. Kyriakopoulos, "EMG-Based Control of a Robot Arm Using Low-Dimensional Embeddings," *IEEE Trans. Robot.*, vol. 26, no. 2, May. 2010, pp. 393-398.

[3] J. Vogel, C. Castellini, and P. van der Smagt, "EMG-based teleoperation and manipulation with the DLR LWR-III," in *Proc. IEEE/RSJ Int. Conf. Intell. Robots Syst. (IROS)*, Sep. 2011, pp. 675-678.

[4] A. H. Al-Timemy, R. N. Khushaba, G. Bugmann, and J. Escudero, "Improving the performance against force variation of EMG controlled multifunctional upper-limb prostheses for transradial amputees," *IEEE Trans. Neural Syst. Rehabil. Eng*., vol. 24, pp. 650-661, 2016.

[5] R. N. Khushaba, S. Kodagoda, "Electromyogram (EMG) feature reduction using mutual components analysis for multifunction prosthetic fingers control," In *Proc. 12th Int. Conf. Control Autom. Robot. Vis*. Dec. 2012, pp. 1534-1539.

[6] L. Dipietro, M. Ferraro, J. J. Palazzolo, H. I. Krebs, B. T. Volpe, and N. Hogan, "Customized interactive robotic treatment for stroke: EMG-triggered therapy," *IEEE Trans. Neural Syst. Rehabil. Eng.*, vol. 13, pp. 325-334, 2005.

[7] S. W. Lee, K. M. Wilson, B. A. Lock, and D. G. Kamper, "Subject-specific myoelectric pattern classification of functional hand movements for stroke survivors," *IEEE Trans. Neural Syst. Rehabil. Eng.*, vol. 19, pp. 558-566, 2011.

[8] K. Englehart and B. Hudgins, "A robust, real-time control scheme for multifunction myoelectric control," *IEEE Trans. Biomed. Eng.*, vol. 50, no. 7, pp. 848-854, 2003.

[9] E. Scheme and K. Englehart, "Electromyogram pattern recognition for control of powered upper-limb prostheses: state of the art and challenges for clinical use," *J. Rehabil. Res. Dev*., vol. 48, no. 6, pp. 643-659, 2011.

[10] P. K. Artemiadis and K. J. Kyriakopoulos, "An EMG-based robot control scheme robust to time-varying EMG signal features," *IEEE Trans. Inf. Technol. Biomed.*, vol. 14, no. 3, pp. 582-588, 2010.

[11] J. Vogel, J. Bayer, and P. van der Smagt, "Continuous robot control using surface electromyography of atrophic muscles," in *Proc. IEEE Int. Conf. Intell. Robots Syst.*, Nov. 3, 2013, pp. 845-850.

[12] A. J. Young, L. H. Smith, E. J. Rouse, and L. J. Hargrove, "Classification of simultaneous movements using surface EMG

pattern recognition," *IEEE Trans. Biomed. Eng*., vol. 60, no. 5, pp. 1250-1258, 2012.

[13] A. B. Ajiboye and R. F. Weir, "A heuristic fuzzy logic approach to EMG pattern recognition for multifunctional prosthesis control," *IEEE Trans. Neural Syst. Rehabil. Eng*., vol. 13, no. 3, pp. 280-291, 2005.

[14] J.-U. Chu, I. Moon, Y.-J. Lee, S.-K. Kim, and M.-S. Mun, "A supervised feature-projection-based real-time EMG pattern recognition for multifunction myoelectric hand control," *IEEE/ASME Trans. Mechatronics*, vol. 12, pp. 282-290, 2007.

[18] W. Geng, Y. Du, W. Jin, W. Wei, Y. Hu, J. Li, "Gesture recognition by instantaneous surface EMG images," *Sci. Rep*., vol. 6, p. 36571, 2016.

[19] X. Zhai, B. Jelfs, R. H. M. Chan, and C. Tin, "Self-recalibrating surface EMG pattern recognition for neuroprosthesis control based on convolutional neural network," *Front. Neurosci.*, vol. 11, p. 379, 2017.

[20] N. A. Shrirao, N. P. Reddy, D. R. Kosuri, "Neural network committees for finger joint angle estimation from surface EMG signals," *Biomed. Eng. Online*, vol. 8, p. 2, 2009.

[21] M. Hioki and H. Kawasaki, "Estimation of finger joint angles from sEMG using a recurrent neural network with time-delayed input vectors," in *Proc. IEEE Int. Conf. Rehabil. Robot. (ICORR)*, July 26, 2009, pp. 289-294.

[22] J. G. Ngeo et al., "Control of an optimal finger exoskeleton based on continuous joint angle estimation from EMG signals," in *Annu. Int. Conf. IEEE Eng. Med. Biol. Soc. (EMBC)*, 2013, pp. 338-341.

[23] J. G. Ngeo, T. Tamei, T. Shibata, "Continuous and simultaneous estimation of finger kinematics using inputs from an EMG-to-muscle activation model," *J. Neuroeng. Rehabil*., vol. 11, p. 122, Aug. 2014.

[24] C. Dai and X. Hu, "Finger joint angle estimation based on motoneuron discharge activities," *IEEE J. Biomed. Health Inform*., vol. 24, no. 3, pp. 760-767, 2020.

[25] W. Guo, C. Ma, Z. Wang, H. Zhang, D. Farina, N. Jiang, and C. Lin, "Long exposure convolutional memory network for accurate estimation of finger kinematics from surface electromyographic signals," *J. Neural Eng*., vol. 18, no. 2, 026020, 2021.

[26] Y. Geng, Z. Yu, Y. Long, L. Qin, Z. Chen, Y. Li, X. Guo, and G. Li., "A CNN-attention network for continuous estimation of finger kinematics from surface electromyograms," *IEEE Robot. Autom. Lett*., vol. 7, no. 3, pp. 6297-6304, 2022.

[27] Y. Chen, S. Yu, K. Ma, S. Huang, G. Li, S. Cai, and L. Xie, "A Continuous estimation model of upper limb joint angles by using surface electromyography and deep learning method," *IEEE Access*, vol. 7, pp. 174940-174950, 2019.

[28] H. Wang, T. Qing, S. Na, and X. Zhang, "Simultaneous estimation of hand joints' angles toward sEMG-driven human–robot interaction," *IEEE Access*, vol. 10, pp. 109385-109394.

[29] K. J. Cole and J. H. Abbs, "Coordination of three-joint digit movements for rapid finger-thumb grasp," *J. Neurophysiol*., vol. 55, no. 6, pp. 1407-1423, 1986.

[30] U. Arnet, D. A. Muzykewicz, J. Fridén, and R. L. Lieber, "Intrinsic hand muscle function, part 1: creating a functional grasp," *J. Hand Surg. Am*., vol. 38, no. 11, pp. 2093-2099, 2013.

[31] W. G. Darling, K. J. Cole, and G. F. Miller, "Coordination of index finger movements," *J. Biomech.*, vol. 27, no. 4, pp. 479-491, 1994.

[32] F. J. Valero-Cuevas, J.-W. Yi, D. Brown, R. V. McNamara 3rd, C. Paul, and H. Lipson, "The tendon network of the fingers performs anatomical computation at a macroscopic scale," *IEEE Trans. Biomed. Eng*., vol. 54, no. 6, pp. 1161-1166, 2007.

[33] M. H. Schieber and M. Santello, "Hand function: peripheral and central constraints on performance," *J. Appl. Physiol.*, vol. 96, no. 6, pp. 2293-2300, 2004.

[34] I. V. Grinyagin, E. V. Biryukova, and M. A. Maier, "Kinematic and dynamic synergies of human precision-grip movements," *J. Neurophysiol*, vol. 94, no. 4, pp. 2284-2294, 2005.

[35] T. D. Niehues, P. Rao, and A. D. Deshpande, "Compliance in parallel to actuators for improving stability of robotic hands during grasping and manipulation," *Int. J. Robot. Res.*, vol. 34, pp. 256-269, 2015.

[36] Luo, J., Huang, D., Li, Y. and Yang, C., "Trajectory online adaption based on human motion prediction for teleoperation," *IEEE Trans. Autom. Sci. Eng.*, vol. 19, no. 4, pp.3184-3191, 2021.

[15] G. Li, Y. Li, Z. Zhang, Y. Geng, and R. Zhou, "Selection of sampling rate for EMG pattern recognition-based prosthesis control," in *Proc. Annu. Int. Conf. IEEE Eng. Med. Biol. Soc.*, 2010, pp. 5058-5061.

[16] C. Cipriani, F. Zaccone, S. Micera, and M. C. Carrozza, "On the shared control of an EMG-controlled prosthetic hand: Analysis of user–prosthesis interaction," *IEEE Trans. Robotics*, vol. 24, pp. 170-184, 2008.

[17] A. A. Adewuyi, L. J. Hargrove, and T. A. Kuiken, "An Analysis of Intrinsic and Extrinsic Hand Muscle EMG for Improved Pattern Recognition Control," *IEEE Trans. Neural Syst. Rehabil. Eng.*, vol. 24, no. 4, pp. 485-494, 2016.

[37] Du, Z., Wang, W., Yan, Z., Dong, W. and Wang, W., "Variable admittance control based on fuzzy reinforcement learning for minimally invasive surgery manipulator," sensors, vol. 17, no. 4, p.844, 2017.

[38] D. L. Crouch and H. Huang, "Lumped-parameter electromyogram-driven musculoskeletal hand model: A potential platform for real-time prosthesis control," *J. Biomech.*, vol. 49, no. 16, pp. 3901-3907, 2016.

[39] L. Pan, D. L. Crouch, and H. Huang, "Comparing EMG-Based Human-Machine Interfaces for Estimating Continuous, Coordinated Movements," *IEEE Trans Neural Syst. Rehabil. Eng*., vol. 27, no. 10, pp. 2145-2154, 2019.

[40] Z. Zhang, M. W. Beck, D. A. Winkler, B. Huang, W. Sibanda, H. Goyal, et al., "Opening the black box of neural networks: methods for interpreting neural network models in clinical applications," *Ann Transl Med*, vol. 6, no. 11, p. 216, 2018.

[41] L. M. Dang, H. Wang, Y. Li, and T. Nguyen, "Explainable artificial intelligence: a comprehensive review," *Artif. Intell. Rev*., vol. 55, pp. 3503-3568, 2022.

[42] X. Liu, K. M. Mosier, F. A. Mussa-Ivaldi, M. Casadio, and R. A. Scheidt, "Reorganization of finger coordination patterns during adaptation to rotation and scaling of a newly learned sensorimotor transformation," *J. Neurophysiol.*, vol. 105, no. 1, pp. 454-473, 2011.

[43] S. W. Lee and D. G. Kamper, "Modeling of multiarticular muscles: importance of inclusion of tendon-pulley interactions in the finger," *IEEE Trans. Biomed. Eng.*, vol. 56, no. 9, pp. 2253-2262, 2009.

[44] T. S. Buchanan, D. G. Lloyd, K. Manal, and T. F. Besier, "Neuromusculoskeletal modeling: estimation of muscle forces and joint moments and movements from measurements of neural command," *J. Appl. Biomech*., vol. 20, no. 4, pp. 367-395, 2004.

[45] C. Ma, C. Lin, O. W. Samuel, W. Guo, H. Zhang, S. Greenwald, L. Xu, and G. Li, "A bi-directional LSTM network for estimating continuous upper limb movement from surface electromyography," *IEEE Robot. Autom. Lett.*, vol. 6, pp. 7217-7224, 2021.

[46] C. Wang, W. Guo, H. Zhang, L. Guo, C. Huang, and C. Lin, "sEMG-based continuous estimation of grasp movements by long-short term memory network," *Biomed. Signal Process. Control*, vol. 59, p. 101774, 2020.

[47] D. Kingma and J. Ba, "Adam: A Method for Stochastic Optimization," *arXiv preprint arXiv*:1412.6980. 2014.

[48] D. G. Kamper, T. G. Hornby, and W. Z. Rymer, "Extrinsic flexor muscles generate concurrent flexion of all three finger joints," *J. Biomech*., vol. 35, no. 12, pp. 1581-1589, 2002.

[49] P. H. Kuo and A. D. Deshpande, "Muscle-tendon units provide limited contributions to the passive stiffness of the index finger metacarpophalangeal joint," *J. Biomech.*, vol. 45, no. 15, pp. 2531-2538, 2012.

[50] T. S. Buchanan, D. G. Lloyd, K. Manal, and T. F. Besier, "Neuromusculoskeletal modeling: estimation of muscle forces and joint moments and movements from measurements of neural command," *J. Appl. Biomech.*, vol. 20, no. 4, pp. 367-395, 2004.

[51] J. R. Potvin, "Effects of muscle kinematics on surface EMG amplitude and frequency during fatiguing dynamic contractions," *J. Appl. Physiol.*, vol. 82, no. 1, pp. 144-151, 1997.

[52] D. G. Lloyd and T. F. Besier, "An EMG-driven musculoskeletal model to estimate muscle forces and knee joint moments in vivo," *J. Biomech*., vol. 36, no. 6, pp. 765-776, 2003.

[53] X. Zhang, S. W. Lee, and P. Braido, "Determining finger segmental centers of rotation in flexion-extension based on surface marker measurement," *J. Biomech*., vol. 36, no. 8, pp. 1097-1102, 2003.

[54] A. D. Deshpande, N. Gialias, and Y. Matsuoka, "Contributions of intrinsic viscoelastic torques during planar index finger and wrist

movements," *IEEE Trans. Biomed. Eng*., vol. 59, no. 2, pp. 586-594, 2012.
[55] L. D. Ketchum, D. Thompson, G. Pocock, D. Wallingford. "A clinical study of forces generated by the intrinsic muscles of the index finger and the extrinsic flexor and extensor muscles of the hand," *J. Hand Surg*., vol. 3, pp. 571-578, 1978.
[56] Kozin SH, Porter S, Clark P, Thoder JJ. The contribution of the intrinsic muscles to grip and pinch strength. The Journal of hand surgery. 1999 Jan 1;24(1):64-72.
[57] Charles Long II, Conrad PW, Hall EA, Furler SL. Intrinsic-extrinsic muscle control of the hand in power grip and precision handling: an electromyographic study. JBJS. 1970 Jul 1;52(5):853-67.
[61][60] P. Haggard and A. Wing, "Coordination of hand aperture with the spatial path of hand transport," *Exp. Brain Res.*, vol. 118, no. 2, pp. 286-292, 1998.
[62][61] S. Piana, A. Staglianò, F. Odone, and A. Camurri, "Adaptive Body Gesture Representation for Automatic Emotion Recognition," *ACM Trans. Interact. Intell. Syst.*, vol. 6, pp. 1-31, 2016.
[63][62] F. Ahmed, A. Bari, and M. Gavrilova, "Emotion recognition from body movement," *IEEE Access*, vol. 8, pp. 11761-11781, 2019.
[64][63] K. Kursa, L. Lattanza, E. Diao, and D. Rempel, "In vivo flexor tendon forces increase with finger and wrist flexion during active finger flexion and extension," *J. Orthop. Res.*, vol. 24, no. 4, pp. 763-769, 2006.
[58] T. Niehues, P. Rao, and A. Deshpande, "Compliance in parallel to actuators for improving stability of robotic hands during grasping and manipulation," *Int. J. Robot. Res.*, vol. 34, pp.256-269, 2015.
[59] J. R. Tresilian, G. E. Stelmach, and C. H. Adler, "Stability of reach-to-grasp movement patterns in Parkinson's disease," *Brain*, vol. 120, no. 11, pp. 2093-2111, 1997.
[60] Y. Paulignan, C. MacKenzie, R. Marteniuk, and M. Jeannerod, "The coupling of arm and finger movements during prehension," *Exp. Brain Res*., vol. 79, pp. 431-435, 1990.

TRENTON GILSTRAP received the B.S. degree in bioengineering from the University of Pittsburgh. He is currently pursuing the Ph.D. degree in biomedical engineering at the Catholic University of America, Washington, DC, USA.

Since 2016, he has worked as a Graduate Research Assistant in the Neuromechanics Laboratory at the Catholic University of America. His research interest includes developing and testing mechatronic devices for rehabilitation of upper extremity movements of those with neurological disorders. He has also focused on the design and fabrication of teleoperation devices controlled with surface electromyography.

Mr. Gilstrap was a recipient of the Bill Gates Foundation Millennium Scholarship in 2011.

THANH PHAN received his B.E degree in biomedical engineering from International University of Vietnam National Universities of Ho Chi Minh City, Vietnam, in 2014. He received the M.S. degree in Electrical Engineering from Ulsan National Institute of Science and Technology, Ulsan, Korea in 2018.

He is currently a Ph.D. candidate in Catholic University of America and research assistant at Center for Applied Biomechanics and Rehabilitation Research, MedStar National Rehabilitation, Washington, DC. His current research interests include exoskeleton design and robotic rehabilitation for stroke, human biomechanics and motor control of hand.

MADA M. ALGHAMDI received the B.S. and M.S. degrees in biomedical engineering from the Catholic University of America, Washington, DC, USA, in 2019 and 2020, respectively.

She is currently working toward a Ph.D. degree on passive arm devices and virtual reality technology for effective stroke rehabilitation. She is also involved in other projects that focused on identifying biomechanical and psychological factors that influence arm use post-stroke.

SANG WOOK LEE (Member, IEEE) received the B.S. and M.S. degrees in mechanical design and production engineering from Seoul National University, Seoul, Korea, in 1997 and 1999, respectively, and the Ph.D. degree in mechanical engineering from University of Illinois, Urbana-Champaign, IL, USA, in 2006. From 2006 to 2010, he was a postdoctoral fellow at the Rehabilitation Institute of Chicago (now Shirley Ryan AbilityLab).

He is currently a visiting scholar at the Rehabilitation Medicine Department at the National Institute of Health (NIH) Clinical Center, Bethesda, MD, USA. He is an Associate Professor in the Department of Biomedical Engineering at the Catholic University of America, Washington, DC, USA, and holds a joint appointment as a Research Scientist at the Center for Applied Biomechanics and Rehabilitation Research in the MedStar National Rehabilitation Hospital, Washington, DC, USA, and as an Adjunct Professor in the Department of Mechanical Engineering, Korea Advanced Institute of Science and Technology, Daejeon, Korea. His current research focuses on examining abnormal neuromechanics of the human hand and upper extremity after neurological injuries such as stroke and cerebral palsy, and developing novel engineering methods to promote their functional recovery.